

Quantitative Studies of Apparent Rotational Temperatures of OH in Emission and Absorption (Spectral Lines with Doppler Contour)*

S. S. PENNER

Guggenheim Jet Propulsion Center, California Institute of Technology, Pasadena, California

(Received July 28, 1952)

Even if a Boltzmann distribution exists for the population of molecules in various energy levels, it is not possible to obtain a satisfactory interpretation of experimental data by the use of conventional procedures unless the product of maximum spectral absorption coefficient P_{\max} and optical density X is sufficiently small. Detailed calculations are presented which show that the experimental results, which suggest an anomalous rotational temperature for the ${}^2\Sigma$ state of OH in low pressure combustion flames, can be accounted for by using sufficiently large values for $P_{\max}X$ (Sec. II). Whether or not experimental data should be interpreted in this manner must be determined by auxiliary studies.

Representative absorption studies for the determination of rotational temperatures in isothermal systems have been analyzed for the P_1 branch, (0,0) band, ${}^2\Pi \rightarrow {}^2\Sigma$ transitions of OH at 3000°K. The calculations show that erroneous interpretation of experimental results occurs if the product $P_{\max}X$ is not small compared to unity. Sample calculations for a blackbody light source show that the customary procedure for treating experimental results will permit adequate correlation of the data by straight lines up to relatively large values for $P_{\max}X$. It is remarkable that the preceding statement remains true even under conditions in which emission data clearly indicate that $P_{\max}X$ is no longer small compared to unity (Sec. III).

I. INTRODUCTION

EXPERIMENTAL studies of population temperatures in flames have been reported, by different investigators, for the ${}^2\Sigma \rightarrow {}^2\Pi$ transitions of OH in flames at low pressures^{1,2} and at atmospheric pressures.^{1,3,4} When the experimental data are treated according to conventional techniques,^{1,2,4} the plots that are used for the determination of rotational temperatures are sometimes found to exhibit discontinuities or curvatures both in the regions of small and of large values of the rotational energy $E(K)$ of the initial (upper) state. The "discontinuities" observed for small values of K have been variously attributed to the formation of OH in the excited electronic state by different chemical reactions leading to a bimodal distribution of population densities,^{1,4} to falsification of experimental data by absorption of emitted radiation by cooler gas layers through which the flame is viewed,⁴ and to self-absorption.⁵

* Supported by the ONR under Contract Nonr-220(03), NR 015 210.

¹ A. G. Gaydon and H. G. Wolfhard, Proc. Roy. Soc. (London) A194, 169 (1948); A199, 89 (1949); A201, 561 (1950); A201, 570 (1950); A205, 118 (1951); A208, 63 (1951).

² Penner, Gilbert, and Weber, J. Chem. Phys. 20, 522 (1952). For a detailed description of the low pressure flame apparatus see M. Gilbert, "The Investigation of Low Pressure Flames," Report No. 4-54 (Jet Propulsion Laboratory, Pasadena, August 30, 1949).

³ H. P. Broida and K. E. Shuler, J. Chem. Phys. 20, 168 (1952).

⁴ H. P. Broida, J. Chem. Phys. 19, 1383 (1951).

⁵ G. H. Dieke and H. M. Crosswhite, "The Ultraviolet Bands of OH," The Johns Hopkins University, Bumblebee Series Report No. 87, 1948.

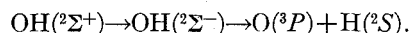
Representative calculations to determine observable peak and total intensity ratios in emission for spectral lines with Doppler contour have been carried out for ${}^2\Sigma \rightarrow {}^2\Pi$ transitions, (0,0) band, P_1 branch of OH at 3000°K. The calculations show that the ratios of peak and total intensities are functions of the products of maximum absorption coefficients (P_{\max}) and optical density (X) for the lines under study (Sec. IV).

Quantitative calculations have been carried out of apparent rotational temperatures in systems containing nonequilibrium distributions of OH at 3000°K and at 6000°K. The calculations on the P_1 branch, ${}^2\Sigma \rightarrow {}^2\Pi$ transitions, indicate that, in the absence of self-absorption, conventional plots showing discontinuities necessarily overestimate one and underestimate the other of the known temperatures of 3000°K and 6000°K (Sec. V).

Quantitative calculations on the nature of distortions produced when an isothermal region at 3000°K is viewed through an isothermal region at 1500°K show that the presence of a non-isothermal field of view magnifies the distortion produced by self-absorption alone (Sec. VI).

On the basis of the noncontroversial quantitative calculations described in Secs. II to VI for idealized systems, some speculations regarding the significance of reported flame temperature anomalies for OH are presented in Sec. VII.

Some of the curvatures observed for large values of K have been interpreted¹ to indicate predissociation according to the process



In a previous publication⁶ we have called attention to the fact that the best available intensity estimates⁷ on OH indicate that the product of the maximum absorption coefficient P_{\max} and of the optical density of the emitters X is not small compared to unity for the more intense spectral lines of OH in representative low pressure flames. In order to obtain reliable quantitative data upon which a rational interpretation of flame spectra can be based, we shall investigate theoretically, as an essential step in the interpretation of flame spectra, the radiation characteristics of various idealized systems both in emission and in absorption.

In Sec. II we examine quantitatively the effect of the size of $P_{\max}X$ on apparent population temperatures in isothermal systems for emission experiments. This study leads us to the conclusion that most of the experimental data *could be* accounted for by a population temperature which is close to the adiabatic flame temperature. Thus, the quantitative calculations are in agreement with Dieke's remarks that the observed discontinuities or curvatures for small values of E_k *may be* the result of self-absorption. Furthermore, an apparent falling off in

⁶ S. S. Penner, J. Chem. Phys. 20, 507 (1952).

⁷ R. J. Dwyer and O. Oldenberg, J. Chem. Phys. 12, 351 (1944); O. Oldenberg and F. F. Rieke, J. Chem. Phys. 6, 439 (1938).

intensity for large values of E_K also *could be* the result, in part, of falsification of experimental data by self-absorption.

In Sec. III we indicate briefly possible effects of large values of $P_{\max}X$ on apparent population temperatures T_i' obtained in absorption experiments for spectral lines with Doppler contour. The results of calculations for ${}^2\Pi \rightarrow {}^2\Sigma$ transitions of OH and the (0,0) band show that the apparent population temperature is strongly dependent on the numerical value of $P_{\max}X$ and relatively insensitive to the temperature of the light source, as long as the source is appreciably hotter than the flame.

In Sec. IV quantitative calculations are described on the influence of absolute values of spectral emissivities on the use of the iso-intensity methods.^{5,8} Representative calculations have been carried out for ${}^2\Sigma \rightarrow {}^2\Pi$ transitions of OH at 3000°K for the (0,0) band and the P_1 branch. The results of the present analysis show that temperature anomalies, obtained by use of the iso-intensity method, *could be* the result of failure to allow for the effect of values of the spectral emissivity on the peak and total intensities of spectral lines with Doppler contour.

In Sec. V the radiation characteristics of a non-equilibrium mixture of OH are investigated in terms of conventional and iso-intensity methods for the interpretation of emission experiments. These calculations show that even for systems without self-absorption the interpretation of experimental data is not unambiguous as long as conventional plots show any deviations from linearity. Furthermore, at least for the P_1 branch, linear iso-intensity plots of the Shuler type are no assurance for thermal equilibrium of the emitter.

In Sec. VI a simplified model is used to study the simultaneous distortion of experimental data by the combined effects of self-absorption and temperature gradients. These studies show that observation of a hot isothermal region through a cooler gas layer accentuates the distortion produced in conventional plots for the interpretation of emission data.

The material presented in Secs. II to VI rests on accepted procedures for the analysis of radiating systems and spectral lines with Doppler contour. The results obtained are not applicable to real flames without conjectures. However, on the basis of the quantitative studies described in Secs. II to VI, some words of caution regarding the acceptance of anomalous population temperatures for OH appear to be justified (Sec. VII).

II. THE EFFECT OF SELF-ABSORPTION ON APPARENT POPULATION TEMPERATURES IN EMISSION EXPERIMENTS

The effect of instrumental distortion on experimental data will be neglected in the present discussion. For the sake of simplicity, a complete analysis will be carried out

only for studies involving peak intensities. It is shown in Appendix I that the results obtained for total intensities, for representative calculations, are similar to those obtained for peak intensities.† Hence, the applicability of the principal conclusions reached in the following discussion depends only on the experimental determination of valid relative peak or integrated intensities for different spectral lines.

A. Equations for the Determination of Apparent Population Temperatures

For spectral lines with Doppler contour the maximum observable intensity in emission I_{\max} is given by the relation

$$I_{\max} = R^0(\nu_{lu})[1 - \exp(-P_{\max}X)], \quad (1)$$

where $R^0(\nu_{lu})$ denotes the intensity of radiation emitted by a blackbody, which is at the same temperature T_u as the gaseous emitters under study, and X is the optical density of the emitter. The frequency ν_{lu} is obtained from the values of the upper (E_u) and lower (E_l) energy levels by use of the Bohr frequency relation. For spectral lines with Doppler contour it is well known that

$$P_{\max} = S_{lu}(mc^2/2\pi kT_i \nu_{lu}^2)^{\frac{1}{2}},$$

where S_{lu} is the integrated intensity for the transition under study, m equals the mass of the radiator, c is the velocity of light, k represents the Boltzmann constant, and T_i is the translational temperature.⁶ Let

$$\epsilon' = I_{\max}/R^0(\nu_{lu}) \quad (2)$$

and $x = -P_{\max}X$, whence it follows that $-\epsilon' = \exp(x) - 1$. It is evident that ϵ' represents the maximum value of the spectral emissivity for the emitted spectral lines.‡ If the population temperature of the emitter is defined in the usual way, then $\epsilon' \leq 1$.

For very small values of ϵ' the well-known result $-x = \epsilon'$ is obtained. From an appropriate expression for S_{lu} it is readily shown that⁶

$$\frac{\partial \ln[I_{\max}/(\nu_{lu})^2 g_u(q_{lu})^2]}{\partial E_u} = -\frac{1}{kT_u} \text{ for } \epsilon' \ll 1, \quad (3)$$

where g_u is the statistical weight of the upper (initial) energy state, q_{lu} is the matrix element for the transition under study, and T_u is the apparent temperature of the upper state involved in the given transition.

If ϵ' is not small compared to unity then it is no longer possible to obtain the value of T_u in a simple manner unless numerical values of ϵ' are available.

† In general, peak intensity ratios are obtained if the instrumental slit width is small compared to the line width, whereas total intensity ratios are measured when the instrumental slit width is large compared to the line width.

‡ Representative values of $\epsilon'(1)$ for low pressure flames lie between 0.3 and 0.90. In order to utilize the data given in Table II of reference 6 for the calculation of $\epsilon'(1)$, care must be taken to use for X the optical density of emitter in the ground level involved in a given transition.

⁸ K. E. Shuler, J. Chem. Phys. 18, 1466 (1950).

B. A Method for Demonstrating the Effect of Self-Absorption on Apparent Population Temperatures of OH (${}^2\Sigma \rightarrow {}^2\Pi$ Transitions)

We proceed now to examine quantitatively the effect of the absolute values of ϵ' on apparent population temperatures determined according to Eq. (3).

Plots of $\log[I_{\max}/(\nu_{lu})^8 g_u(q_{lu})^2]$ as a function of E_u can be constructed for various assumed values of ϵ' by proceeding according to the scheme outlined below.

(1) Assume a value of ϵ' , for example, for the P_1 branch, (0,0) band, for the transition identified by the index $K=1$, using the notation of Dieke and Crosswhite.⁵ It is then evident from Eqs. (1) and (2) that

$$(P_{\max}X)_{K=1} = -2.303 \log[1 - \epsilon'(K=1)]. \quad (4)$$

(2) Calculate the ratio $S_{lu}(K)/S_{lu}(K=1)$ from the expression

$$\frac{S_{lu}(K)}{S_{lu}(K=1)} = \frac{g_u(K)[q_{lu}(K)]^2}{g_u(K=1)[q_{lu}(K=1)]^2} \frac{\nu_{lu}(K)}{\nu_{lu}(K=1)} \times \{\exp[-E_u(K) - E_u(K=1)]/kT\} \times \{\exp[h\nu_{lu}(K)/kT] - 1\} \times \{\exp[h\nu_{lu}(K=1)/kT] - 1\}^{-1}. \quad (5)$$

The first fraction appearing on the right-hand side of Eq. (5) is given by results obtained by Hill and Van Vleck⁹ as written in convenient form by Earls¹⁰ and tabulated by Dieke and Crosswhite.⁵ The quantities $\nu_{lu}(K)$ and $E_u(K)$ have also been tabulated.⁵

(3) Determine $(P_{\max}X)_K$ from the relation

$$(P_{\max}X)_K = (P_{\max}X)_{K=1} \frac{S_{lu}(K)}{S_{lu}(K=1)} \frac{\nu_{lu}(K=1)}{\nu_{lu}(K)}, \quad (6)$$

and evaluate

$$\epsilon'(K) = 1 - \exp(-(P_{\max}X)_K). \quad (7)$$

(4) Calculate

$$(I_{\max})_K = \epsilon'(K)[R^0(\nu_{lu})]_K. \quad (8)$$

TABLE I. Apparent population temperatures T_u' obtained from lines with $10 \leq K \leq 18$ for the P_1 branch, (0,0) band, and ${}^2\Sigma \rightarrow {}^2\Pi$ transitions of OH at 3000°K, as a function of assumed values of $\epsilon'(1)$.^a

| $\epsilon'(1)$ | $T_u', \text{ }^\circ\text{K}$ |
|----------------|--------------------------------|
| 0.1 | 3 000 |
| 0.3 | ~3 200 |
| 0.5 | ~3 500 |
| 0.7 | ~5 000 |
| 0.9 | ~6 500 |
| 0.95 | ~10 000 |
| 0.999 | ~19 000 |

^a For representative flames: $0.3 \leq \epsilon'(1) \leq 0.90$.

⁹ E. Hill and J. H. Van Vleck, Phys. Rev. **32**, 250 (1928).

¹⁰ L. T. Earls, Phys. Rev. **48**, 423 (1935).

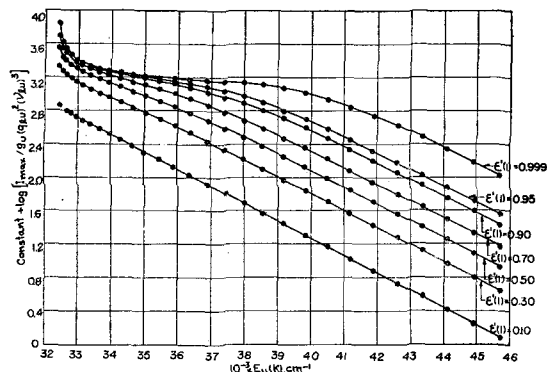


FIG. 1. Conventional plots for the determination of rotational temperatures of OH in emission for various assumed values of $\epsilon'(1)$ for the P_1 branch, ${}^2\Sigma \rightarrow {}^2\Pi$ transitions, (0,0) band, $T=3000^\circ\text{K}$.

(5) Finally calculate $\log(I_{\max})_K - \log\{g_u(K)[q_{lu}(K)]^2 \times [\nu_{lu}(K)]^8\}$, and plot this quantity as a function of $E_u(K)$. From the slope of this plot determine the apparent population temperature T_u' in the usual way by applying Eq. (3).

The results of calculations carried out according to the scheme outlined above are summarized in Fig. 1 for the P_1 branch for various assumed values of $\epsilon'(1)$.

C. Discussion of Results

Analysis of the data listed in Fig. 1 leads to the conclusions enumerated below.

(1) For sufficiently small values of $\epsilon'(1)$, the apparent and true values of the population temperatures are identical since Eq. (3) applies in good approximation. This result is, of course, well known.

(2) As the value of $\epsilon'(1)$ is increased, the plots constructed according to Eq. (3) show increasing curvature for the more intense rotational lines until for $\epsilon'(1)=0.5$ and greater the constructed curves simulate population temperatures which are of the same order of magnitude as the anomalous values reported for flames. It is easy to see how a limited number of experimental points between $K=3$ and $K=20$ could be correlated by two intersecting straight lines. Apparent population temperatures T_u' obtained for lines with $10 \leq K \leq 18$ for the P_1 branch, (0,0) band, and ${}^2\Sigma \rightarrow {}^2\Pi$ transitions of OH at 3000°K are listed in Table I as a function of the assumed value of $\epsilon'(1)$.

(3) For sufficiently large values of K , all of the curves become parallel independently of the assumed values of $\epsilon'(1)$. Thus, all of the experimental data yield apparent population temperatures which are in agreement with the true value of the population temperature. Hence, by extending experimental studies to sufficiently large values of K , it is always possible to obtain unambiguous estimates of the true population temperature.

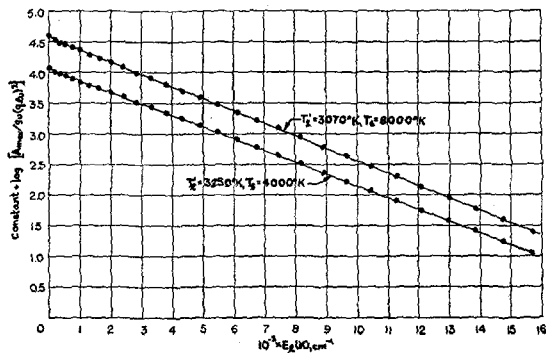


Fig. 2. Conventional plots for the determination of apparent population temperatures T'_l of the ground electronic state from absorption experiments for different temperatures of the light source T_s [$^2\Pi \rightarrow ^2\Sigma$ transitions of OH, (0,0) band, P_1 branch, $T = 3000^\circ\text{K}$, $\alpha'(1) = 0.10$; the ordinate for the plot at $T_s \approx 8000^\circ\text{K}$ has been reduced by 2.00 relative to the plot for $T_s = 4000^\circ\text{K}$].

III. THE EFFECT OF SELF-ABSORPTION ON APPARENT POPULATION TEMPERATURES IN ABSORPTION EXPERIMENTS

At thermodynamic equilibrium the spectral emissivities and absorptivities arising from a given transition are identical. Hence, it is to be expected that falsification of experimental data in absorption experiments needs to be considered whenever self-absorption is known to be of importance in emission. The following analysis is restricted to the use of peak intensities for the calculation of population temperatures. § Instrumental distortion will be neglected as in Sec. II.

A. Equations for the Determination of Apparent Population Temperatures

In an absorption experiment with a source which is much brighter than the emission lines and which emits the spectral radiant intensity $R_S(\nu)$, the maximum value of the fractional absorbed intensity, $\alpha' = A_{\max}/R_S(\nu_{lu})$, is given by the expression

$$\alpha' = 1 - \exp(-P_{\max}X), \quad (9)$$

and

$$-x = \alpha' [1 + \frac{1}{2}\alpha' + (1/3)(\alpha')^2 + (1/4)(\alpha')^3 + \dots]. \quad (10)$$

For $\alpha' \ll 1$, Eq. (10) reduces to the expression $-x = \alpha'$, where⁶

$$S_{lu}X \approx (8\pi^3 N/3hcQ)\nu_{lu}g_u q_{lu}^2 [\exp(-E_l/kT_l)]. \quad (11)$$

Here T_l is the population temperature of the ground (initial) state in an absorption experiment. From Eq. (11) it is readily shown⁶ that for graybody emitters, with the effective temperature of the source, T_s , large compared to T_l ,

$$\frac{\partial \ln[A_{\max}/g_u q_{lu}^2]}{\partial E_l} = -\frac{1}{kT_l}. \quad (12)$$

It is evident that T_l can, in general, be determined only if absolute values of α' are known.

§ The use of apparent total absorption measurements is discussed briefly in Appendix II.

B. A Method for Demonstrating the Effect of Self-Absorption on Apparent Population Temperatures of OH ($^2\Pi \rightarrow ^2\Sigma$ Transitions)

We proceed to examine quantitatively the effect of absolute values of α' on apparent population temperatures determined according to Eq. (12). Plots of $\log[A_{\max}/g_u(q_{lu})^2]$ as a function of E_l can be constructed by using the following scheme.

(1) Assume a value of α' , for example, for the P_1 branch, (0,0) band, for the transition identified by the index $K = 1$, using the notation of Dieke and Crosswhite.⁵ Next calculate $\alpha'(K)$ by using the same procedure as was used to obtain the maximum values of the spectral emissivity for the line with index K (see Sec. II).

(2) Calculate

$$A_{\max} \approx \alpha'(K)R_S(\nu_{lu}), \quad (13)$$

assuming a blackbody distribution curve for the source

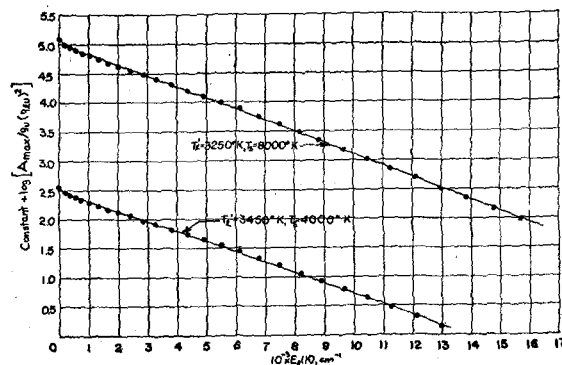


Fig. 3. Conventional plots for the determination of apparent population temperatures T'_l of the ground electronic state from absorption experiments for different temperatures of the light source T_s [$^2\Pi \rightarrow ^2\Sigma$ transitions of OH, (0,0) band, P_1 branch, $T = 3000^\circ\text{K}$, $\alpha'(1) = 0.30$].

at the temperature T_s .

(3) Calculate

$$\log\{(A_{\max})_K/g_u(K)[q_{lu}(K)]^2\}$$

and plot this quantity as a function of $E_l(K)$. From the slope of this plot determine the apparent population temperature T'_l in the usual way by applying Eq. (12).

The results of calculations carried out according to the scheme outlined above are summarized in Figs. 2-5 for $\alpha'(K=1)$ of P_1 branch = 0.1, 0.3, 0.7, and 0.9, respectively, for two or more values of the source temperature T_s . Apparent population temperatures for the relevant assumed conditions are indicated in Figs. 2-5.

C. Discussion of Results

Analysis of the data presented in Figs. 2-5 leads to the conclusions enumerated below.

(1) Experimental data treated according to conventional procedures permit correlation of results by

linear plots even for values of $\alpha'(K=1)$ of the P_1 branch which are so large that T_l' differs appreciably from T_l . Hence, absolute values obtained for T_l' cannot be considered to be meaningful without convincing proof that $P_{\max}X$ is sufficiently small for the spectral lines under study to justify conventional treatment of data.

(2) Apparent population temperatures T_l' are always larger than T_l . The difference between T_l' and T_l decreases somewhat as the temperature of the light source is increased for fixed values of $P_{\max}X$. However, the apparent temperatures are relatively insensitive to the numerical values of T_s , decreasing by only a few hundred degrees as T_s is raised from 3500°K to 8000°K.

(3) For sufficiently large values of $\alpha'(K=1)$ for the P_1 branch, discontinuities or curvatures are observed in the conventional plots which are reminiscent of the results obtained in emission experiments (Sec. II).

Adequate care in the interpretation of absorption studies, as well as of emission studies, permits the determination of both the true rotational temperature and of the concentration of the absorbing or emitting species,

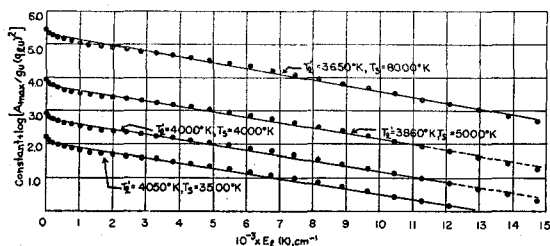


FIG. 4. Conventional plots for the determination of apparent population temperatures T_l' of the ground electronic state from absorption experiments for different temperatures of the light source T_s [$^2\Pi \rightarrow ^2\Sigma$ transitions of OH, (0,0) band, P_1 branch, $T = 3000^\circ\text{K}$, $\alpha'(1) = 0.70$].

provided the population of molecules in the rotational energy levels obeys the Maxwell-Boltzmann distribution law. Thus data on spectral lines with large K can be used to obtain T_l . Next, a family of curves for the known values of T_l and T_s , is constructed, for example, for different values of $\alpha'(K=1)$ for the P_1 branch (compare Figs. 2-5). The data obtained by using Eq. (12) for the lower values of K can then be employed to determine $\alpha'(K=1)$, whence the optical density X is determined since S_{lu} is known.⁷

IV. THE EFFECT OF SELF-ABSORPTION ON THE USE OF ISOINTENSITY METHODS

Serious attempts to correct for the distortion of experimental data produced by self-absorption have been made by Dieke⁵ and his collaborators and also by Shuler.⁸ The limitations of the isointensity method and the care required in its use have been clearly stated by Dieke and Crosswhite.⁵ The quantitative calculations presented here emphasize the fact that it is easy to

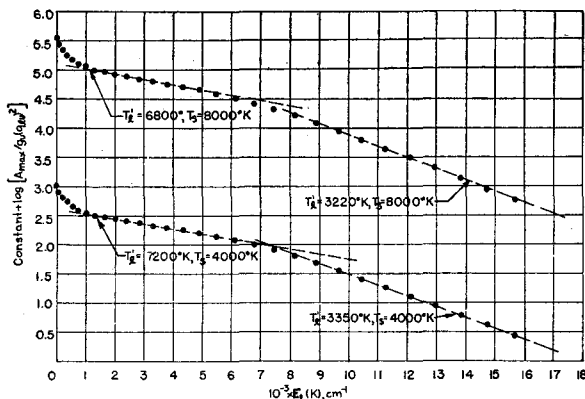


FIG. 5. Conventional plots for the determination of apparent population temperatures T_l' of the ground electronic state from absorption experiments for different temperatures of the light source T_s [$^2\Pi \rightarrow ^2\Sigma$ transitions of OH, (0,0) band, P_1 branch, $T = 3000^\circ\text{K}$, $\alpha'(1) = 0.90$].

obtain erroneous results if isointensity methods are used for the P_1 branch. It is clear that the errors will be smaller but not negligible if the isointensity methods are used for the R_2 branch, as originally proposed by Dieke and Crosswhite.⁵

A. Outline of Calculations

Two spectral lines, which are differentiated by the indices K and K' , appear to have equal peak intensities I_{\max} in an emission experiment, if

$$I_{\max}(K) = I_{\max}(K'), \quad (14)$$

where I_{\max} is given by Eq. (1). For various assumed values of $\epsilon'(K=1)$ of the P_1 branch at 3000°K, it is a simple matter to calculate the ratios $I_{\max}(K)/I_{\max}(K=1)$ by following the procedure described in Sec. II. The results of these calculations are summarized in Table II, and representative values are plotted in Fig. 6.

The spectral lines, which are identified by the indices K and K' , appear to have equal total intensities in emission if

$$A(K) = A(K'), \quad (15)$$

where

$$A(K) = [R\nu_{lu}^0 (mc^2/2\pi kT_l)^{-3/2} \nu_{lu}(K)] [P_{\max}(K)X] \times \sum_{n=0}^{\infty} [(n+1)^2(n+1)!]^{-1} [-P_{\max}(K)X]^n. \quad (16)$$

By proceeding according to the method described in Appendix I, it is readily shown that

$$A(K)/A(K') = [I_{\max}(K)/I_{\max}(K')] \times [\nu_{lu}(K)/\nu_{lu}(K')] [\xi(K')/\xi(K)]. \quad (17)$$

Representative numerical values of $A(K)/A(K')$ are listed in Table III and plotted in Fig. 7 for $^2\Sigma \rightarrow ^2\Pi$ transitions of OH at 3000°K for the (0,0) band and the P_1 branch.

TABLE II. Numerical values of $S_{lu}(K)/S_{lu}(1)$ and of $I_{\max}(K)/I_{\max}(1)$ as a function of $\epsilon'(K=1)$ for the P_1 branch, (0,0) band, ${}^2\Sigma \rightarrow {}^2\Pi$ transitions of OH at 3000°K.

| K | $S_{lu}(K)/S_{lu}(1)$ | $I_{\max}(K)/I_{\max}(1)$ for | | | | | | |
|----|-----------------------|-------------------------------|--------------------|--------------------|--------------------|--------------------|---------------------|---------------------|
| | | $\epsilon'(1)=0.1$ | $\epsilon'(1)=0.3$ | $\epsilon'(1)=0.5$ | $\epsilon'(1)=0.7$ | $\epsilon'(1)=0.9$ | $\epsilon'(1)=0.95$ | $\epsilon'(1)=0.99$ |
| 1 | 1.00 | 1.00 | 1.00 | 1.00 | 1.00 | 1.00 | 1.00 | 1.00 |
| 2 | 1.29 | 1.30 | 1.26 | 1.21 | 1.15 | 1.08 | 1.05 | 1.03 |
| 3 | 1.59 | 1.60 | 1.50 | 1.39 | 1.27 | 1.13 | 1.08 | 1.05 |
| 4 | 1.83 | 1.86 | 1.70 | 1.53 | 1.35 | 1.16 | 1.11 | 1.07 |
| 5 | 2.00 | 2.05 | 1.85 | 1.63 | 1.41 | 1.19 | 1.14 | 1.09 |
| 6 | 2.09 | 2.18 | 1.95 | 1.70 | 1.45 | 1.22 | 1.16 | 1.11 |
| 7 | 2.11 ^a | 2.25 ^a | 2.00 | 1.74 | 1.49 | 1.25 | 1.19 | 1.14 |
| 8 | 2.05 | 2.25 ^a | 2.02 ^a | 1.77 ^a | 1.52 | 1.27 | 1.22 | 1.17 |
| 9 | 1.94 | 2.20 | 1.99 | 1.77 ^a | 1.53 | 1.30 | 1.24 | 1.19 |
| 10 | 1.79 | 2.09 | 1.93 | 1.74 | 1.54 ^a | 1.33 | 1.27 | 1.22 |
| 11 | 1.61 | 1.94 | 1.84 | 1.69 | 1.53 | 1.35 | 1.30 | 1.26 |
| 12 | 1.41 | 1.77 | 1.72 | 1.62 | 1.51 | 1.37 | 1.33 | 1.29 |
| 13 | 1.21 | 1.58 | 1.57 | 1.52 | 1.46 | 1.38 ^a | 1.35 | 1.32 |
| 14 | 1.02 | 1.38 | 1.41 | 1.40 | 1.39 | 1.37 | 1.37 ^a | 1.36 |
| 15 | 0.842 | 1.19 | 1.24 | 1.26 | 1.29 | 1.34 | 1.36 | 1.38 |
| 16 | 0.681 | 1.00 | 1.06 | 1.11 | 1.17 | 1.28 | 1.33 | 1.40 ^a |
| 17 | 0.541 | 0.824 | 0.896 | 0.956 | 1.04 | 1.20 | 1.27 | 1.39 |
| 18 | 0.421 | 0.664 | 0.740 | 0.804 | 0.899 | 1.08 | 1.18 | 1.34 |
| 19 | 0.323 | 0.534 | 0.600 | 0.662 | 0.757 | 0.954 | 1.06 | 1.26 |
| 20 | 0.244 | 0.419 | 0.477 | 0.533 | 0.621 | 0.812 | 0.926 | 1.15 |
| 21 | 0.181 | 0.323 | 0.373 | 0.421 | 0.498 | 0.672 | 0.780 | 1.00 |
| 22 | 0.132 | 0.246 | 0.286 | 0.326 | 0.391 | 0.540 | 0.637 | 0.847 |
| 23 | 0.0954 | 0.185 | 0.217 | 0.249 | 0.301 | 0.424 | 0.506 | 0.690 |
| 24 | 0.0678 | 0.137 | 0.162 | 0.186 | 0.227 | 0.325 | 0.391 | 0.545 |
| 25 | 0.0475 | 0.1004 | 0.119 | 0.138 | 0.169 | 0.244 | 0.296 | 0.419 |
| 26 | 0.0328 | 0.0723 | 0.0868 | 0.100 | 0.123 | 0.180 | 0.219 | 0.314 |
| 27 | 0.0224 | 0.0517 | 0.0618 | 0.0721 | 0.0889 | 0.131 | 0.160 | 0.231 |
| 28 | 0.0151 | 0.0364 | 0.0442 | 0.0511 | 0.0632 | 0.0933 | 0.115 | 0.166 |
| 29 | 0.0101 | 0.0257 | 0.0312 | 0.0359 | 0.0447 | 0.0623 | 0.0814 | 0.119 |
| 30 | 0.0067 | 0.0177 | 0.0219 | 0.0252 | 0.0312 | 0.0462 | 0.0568 | 0.0831 |

^a Maximum intensity ratios.

B. Discussion of Results

Reference to the data listed in Tables II and III and plotted in Figs. 6 and 7 shows that the ratios $I_{\max}(K)/I_{\max}(K')$ and $A(K)/A(K')$ are functions of the values of

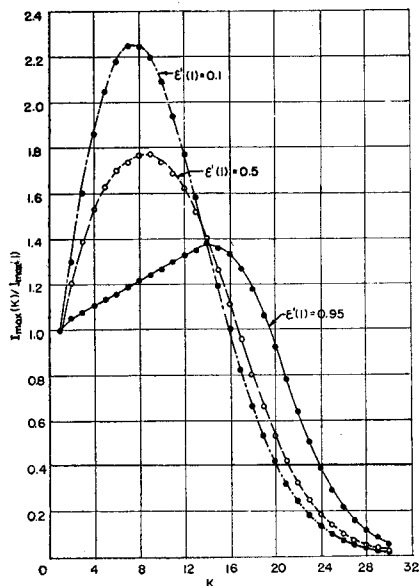


FIG. 6. The ratio $I_{\max}(K)/I_{\max}(1)$ as a function of K for the P_1 branch, (0,0) band, ${}^2\Sigma \rightarrow {}^2\Pi$ transitions of OH at 3000°K for different values of $\epsilon'(1)$.

TABLE III. Representative numerical values of $A(K)/A(1)$ as a function of $\epsilon'(K=1)$ for the P_1 branch, (0,0) band, ${}^2\Sigma \rightarrow {}^2\Pi$ transitions of OH at 3000°K.

| K | $A(K)/A(1)$ for | | | |
|----|--------------------|--------------------|--------------------|---------------------|
| | $\epsilon'(1)=0.1$ | $\epsilon'(1)=0.5$ | $\epsilon'(1)=0.9$ | $\epsilon'(1)=0.95$ |
| 1 | 1.00 | 1.00 | 1.00 | 1.00 |
| 2 | 1.31 | 1.24 | 1.15 | 1.11 |
| 3 | 1.61 | 1.47 | 1.25 | 1.20 |
| 4 | 1.88 | 1.64 | 1.34 | 1.27 |
| 5 | 2.07 | 1.77 | 1.39 | 1.32 |
| 6 | 2.21 | 1.86 | 1.43 | 1.36 |
| 7 | 2.27 | 1.90 | 1.47 | 1.39 |
| 8 | 2.26 | 1.91 | 1.49 | 1.41 |
| 9 | 2.20 | 1.90 | 1.50 | 1.43 |
| 10 | 2.08 | 1.84 | 1.51 | 1.43 |
| 11 | 1.93 | 1.76 | 1.50 | 1.43 |
| 12 | 1.75 | 1.65 | 1.47 | 1.42 |
| 13 | 1.55 | 1.52 | 1.42 | 1.39 |
| 14 | 1.35 | 1.37 | 1.35 | 1.35 |
| 15 | 1.15 | 1.21 | 1.27 | 1.28 |
| 16 | 0.968 | 1.05 | 1.16 | 1.19 |
| 17 | 0.793 | 0.888 | 1.04 | 1.08 |
| 18 | 0.636 | 0.736 | 0.902 | 0.959 |
| 19 | 0.509 | 0.599 | 0.772 | 0.828 |
| 20 | 0.397 | 0.477 | 0.635 | 0.696 |
| 21 | 0.305 | 0.373 | 0.515 | 0.569 |
| 22 | 0.232 | 0.286 | 0.405 | 0.454 |
| 23 | 0.173 | 0.217 | 0.313 | 0.352 |
| 24 | 0.128 | 0.161 | 0.237 | 0.269 |
| 25 | 0.0935 | 0.119 | 0.176 | 0.201 |
| 26 | 0.0671 | 0.0859 | 0.129 | 0.147 |
| 27 | 0.0478 | 0.0615 | 0.0927 | 0.107 |
| 28 | 0.0335 | 0.0433 | 0.0657 | 0.0757 |
| 29 | 0.0236 | 0.0304 | 0.0463 | 0.0536 |
| 30 | 0.0161 | 0.0212 | 0.0321 | 0.0372 |

$\epsilon'(K=1)$ for the P_1 branch, the dependence on $\epsilon'(K=1)$ becoming stronger as $\epsilon'(K=1)$ approaches unity, i.e., as the extent of self-absorption increases. This observation is emphasized by noting, for example, that the line having absolute peak intensity closest to the line with $K=3$, has $K=13$ for $\epsilon'(1)=0.1$, $K=13$ for $\epsilon'(1)=0.3$, $K=14$ for $\epsilon'(1)=0.5$, $K=15$ for $\epsilon'(1)=0.7$, $K=18$ for $\epsilon'(1)=0.9$, $K=19$ for $\epsilon'(1)=0.95$, and $K=21$ for $\epsilon'(1)=0.99$. Comparison of the data given in Tables II and III and plotted in Figs. 6 and 7, respectively, also shows that the effect of self-absorption in falsifying the data obtained by use of the iso-intensity method is more pronounced for peak emitted intensities than for total intensities.

The effect of self-absorption on population temperatures determined from the iso-intensity method can be demonstrated graphically by using the procedure de-

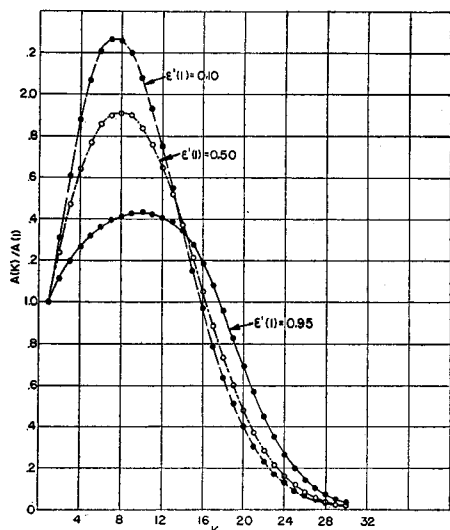


FIG. 7. The ratio $A(K)/A(1)$ as a function of K for the P_1 branch, (0,0) band, ${}^2\Sigma \rightarrow {}^2\Pi$ transitions of OH at 3000°K for different values of $\epsilon'(1)$.

veloped by Shuler⁸ whose method is equivalent to the assumption that total intensity ratios $A(K)/A(K')$ can be replaced by the product of transition probability ratios $g_u(K)[q_{lu}(K)]^2/g_u(K')[q_{lu}(K')]^2$ and appropriate exponential factors for spectral lines which are close together. Plots of $E(K) - E(K')$ vs $\log\{g_u(K)[q_{lu}(K)]^2/g_u(K')[q_{lu}(K')]^2\}$ are shown in Fig. 8 as a function of $\epsilon'(1)$ for pairs of spectral lines for which $I_{\max}(K)/I_{\max}(K')$ is nearly equal to unity. Similarly, plots of $E(K) - E(K')$ vs $\log\{g_u(K)[q_{lu}(K)]^2/g_u(K')[q_{lu}(K')]^2\}$ are shown in Fig. 9 as a function of $\epsilon'(1)$ for pairs of spectral lines for which $A(K)/A(K')$ is nearly equal to unity.

Reference to Figs. 8 and 9 shows that the plots deviate progressively more from straight lines as $\epsilon'(1)$ is increased. Apparent population temperatures T_u' are noted on the curves given in Figs. 8 and 9. The results are seen to be an immediate consequence of the de-

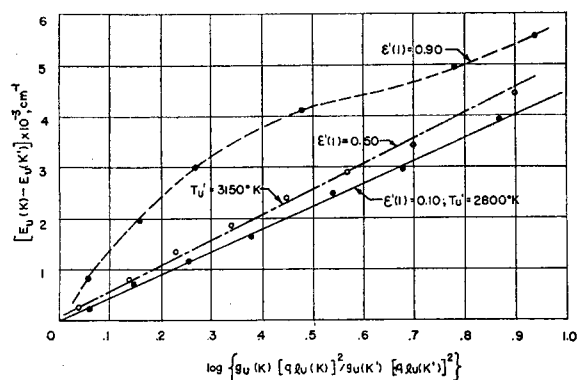


FIG. 8. Plot of $[E_u(K) - E_u(K')] \times [q_{lu}(K)]^2/g_u(K) \times [q_{lu}(K')]^2$ for lines with equal peak intensities at 3000°K as a function of $\epsilon'(1)$ for the P_1 branch, (0,0) band, ${}^2\Sigma \rightarrow {}^2\Pi$ transitions of OH.

pendence of the K values for lines with equal peak or total intensities on $\epsilon'(1)$. Hence, the conclusion is reached that the effects of self-absorption in distorting experimental data do not necessarily cancel in first order for the iso-intensity methods. A simple physical explanation for failure of the iso-intensity methods at large values of the spectral emissivity is obtained by noting that the quantities $R^0(\nu_{lu})$ influence the observable intensities and that $R^0(\nu_{lu})$, which is a function of temperature, is not the same for any distinguishable pair of spectral lines. Furthermore, equally intense spectral lines, for which $S_{lu}(K) = S_{lu}(K')$, have slightly different widths since the Doppler width is proportional to the frequency of the line center. Thus, the obvious conclusion is reached that the effects of self-absorption will cancel exactly only for equally intense spectral lines with line centers occurring at identical frequencies.

V. ERRORS IN CONVENTIONAL PROCEDURES FOR ISOTHERMAL SYSTEMS IN THE ABSENCE OF SELF-ABSORPTION

Whereas the effect of self-absorption in producing distortion of emission data has been amply discussed, relatively little analytical work has been done on the meaning of discontinuous curves for a mixture of

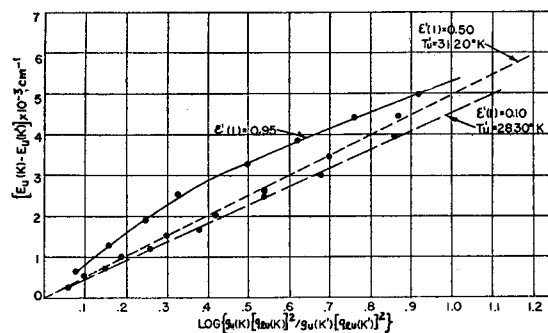


FIG. 9. Plot of $[E_u(K) - E_u(K')] \times [q_{lu}(K)]^2/g_u(K) \times [q_{lu}(K')]^2$ for lines with equal total intensities at 3000°K as a function of $\epsilon'(1)$ for the P_1 branch, (0,0) band, ${}^2\Sigma \rightarrow {}^2\Pi$ transitions of OH.

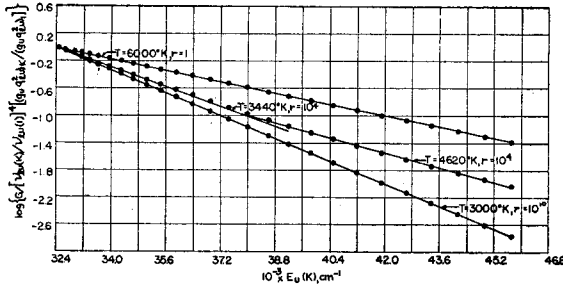


FIG. 10. Conventional plots and apparent temperatures for various bimodal distributions of OH.

isothermal systems in the absence of self-absorption. Although the methods of calculation that we employ are well-known and the conclusions to which they lead are almost obvious, it is somewhat surprising to note that errors in interpretation can be made even for the often-postulated nonequilibrium distribution of OH. Aside from emphasizing the need for care in dealing with anything other than a linear plot, the present analysis also serves to give examples of linear isointensity plots of the Shuler type⁸ for the P_1 branch with meaningless temperatures for a nonequilibrium distribution of OH. Whether or not the R_2 branch is quite as bad can be said with assurance only after quantitative calculations have been carried out; however, we expect the errors to be less pronounced. In this connection reference should be made also to the discussion of the isointensity method given by Dieke and Crosswhite,⁵ who indicate very clearly under what conditions the method is usable.

A. Outline of Theory

For a nonequilibrium mixture of gases containing OH at 3000°K and at 6000°K, the total observable intensity $A(K)$ emitted from the spectral line identified by the index K with line center at $\nu_{lu}(K)$ is given by the expression

$$A(K)/(c/4) = \{ \rho^0[\nu_{lu}(K)] S_{lu}(K) X \}_{T=3000^\circ\text{K}} + \{ \rho^0[\nu_{lu}(K)] S_{lu}(K) X \}_{T=6000^\circ\text{K}}, \quad (18)$$

where $\rho^0[\nu_{lu}(K)]$ is the volume density of radiation emitted by a blackbody at $\nu_{lu}(K)$ and the effects of self-absorption have been assumed to be negligible. The total intensity of the line with index K divided by the total intensity of the line with index $K=1$ is

$$G = A(K)/A(1) = [B(T=6000) + B(T=3000)C]/(1+C), \quad (19)$$

where

$$B(T) = \{ \rho^0[\nu_{lu}(K)] S_{lu}(K) / \rho^0[\nu_{lu}(1)] S_{lu}(1) \}_T = [\nu_{lu}(K)/\nu_{lu}(1)]^4 [(g_u q_{lu^2})_K / (g_u q_{lu^2})_1] \times \exp\{ -[E_u(K) - E_u(1)]/kT \} \quad (20)$$

and

$$C = \{ \rho^0[\nu_{lu}(1)] S_{lu}(1) X \}_{T=3000} / \{ \rho^0[\nu_{lu}(1)] S_{lu}(1) X \}_{T=6000} = (X_{3000}/X_{6000}) \times [\exp\{ -[E_u(1)/k] [(1/3000) - (1/6000)] \}]. \quad (21)$$

The nonequilibrium character of the OH distribution is expressed by

$$r = X_{3000}/X_{6000}. \quad (22)$$

For $r=0$ the present discussion reduces to the analysis of an isothermal system at 6000°K, whereas for $1/r=0$, the radiation becomes that characteristic of an isothermal system at 3000°K. It is apparent that r must be considerably greater than unity before the OH with rotational temperature at 3000°K will influence the observed radiation from the nonequilibrium mixture.

The apparent temperatures which would be obtained from observations of the mixture if conventional treatment of emission data were employed is obtained by plotting $\log\{G/[\nu_{lu}(K)/\nu_{lu}(1)]^4 [(g_u q_{lu^2})_K / (g_u q_{lu^2})_1]\}$ as a function of $E_u(K)$. Similarly, isointensity plots may be constructed according to the method of Shuler⁸ by noting that for equally intense lines with indexes K and K' , respectively, $G(K) = G(K')$.

B. Discussion of Results

Interpretation of measurable intensities according to conventional procedures for analysis of emission data is illustrated in Figs. 10 and 11. In accord with expectations, we find for $r \leq 10^2$ that the observable intensity ratios are practically those characteristic of an isothermal system at 6000°K. On the other hand, for $r \geq 10^6$, the nonequilibrium mixture radiates almost like an isothermal system at 3000°K. For intermediate values of r , numerical values are obtained in the usual logarithmic plots (see Figs. 10 and 11) which can be represented, in adequate approximation, by two intersecting straight lines. For low values of K temperatures greater than 3000°K are obtained, whereas for high values of K temperatures lower than 6000°K are obtained. Of particular interest is the fact that data calculated according to Shuler's isointensity method (see Figs. 12 and 13) can be correlated by linear plots even under conditions in which conventional procedures clearly show discontinuities. Of course, the slopes

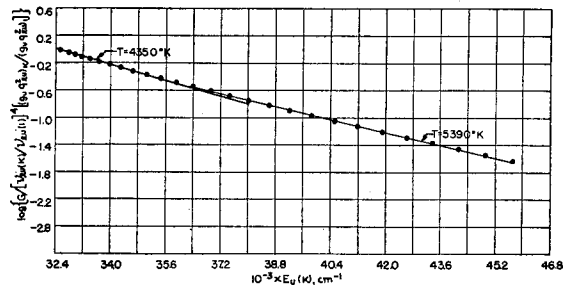


FIG. 11. Conventional plot and apparent temperatures for $r = 2 \times 10^3$.

There are several obvious reasons for this result. Thus, without applying a suitable frequency correction or using interpolation between listed values of K , there is considerable intrinsic scatter in the isointensity plots. Furthermore, the number of points which can be used to draw the final plot is reduced to one-half. Hence, it is quite possible to obtain isointensity plots which do not show the finer details of conventional plots.

derived from Shuler's isointensity plots are meaningless in these cases. These results certainly indicate that as long as nonlinear plots are obtained a simple interpretation of observable data is inadmissible even for a mixture of isothermal systems in the absence of self-absorption. Thus, two intersecting straight lines with apparent temperatures T_1 and T_2 can be obtained only by non-equilibrium mixtures at temperatures other than T_1 and T_2 .

VI. APPARENT TEMPERATURES FOR TWO ADJACENT ISOTHERMAL REGIONS

The observable radiation from real flames is always produced from a nonisothermal field of view. Without a detailed prescription of temperature and concentration gradients along the line of sight, it is not possible to incorporate quantitative corrections in the interpretation of experimental data. However, it is apparent that the falsification of data in conventional plots will be similar to the falsification produced by self-absorption as long as a hot region is viewed through a cooler gas layer. We shall demonstrate this conclusion by representative calculations on the observable emitted radiation for spectral lines with Doppler contour when an isothermal region at 3000°K is viewed through an isothermal region at 1500°K. The concentrations of emitter in the two regions will be treated as variable parameters. Although we present theoretical results only for the P_1 branch, it is clear from a study of the factors responsible for distortions produced by observations through cooler gas layers that, for example, the R_2 branch will be modified in roughly the same manner as the P_1 branch. Hence, although the use of isointensity methods is advantageous in minimizing the effects of self-absorption for the R_2 branch, the use of the R_2 branch becomes less significant if distortion by temperature gradients is also of importance. It is gratifying to note, however, that the distortions resulting from temperature gradients are reduced if the extent of self-absorption is diminished.

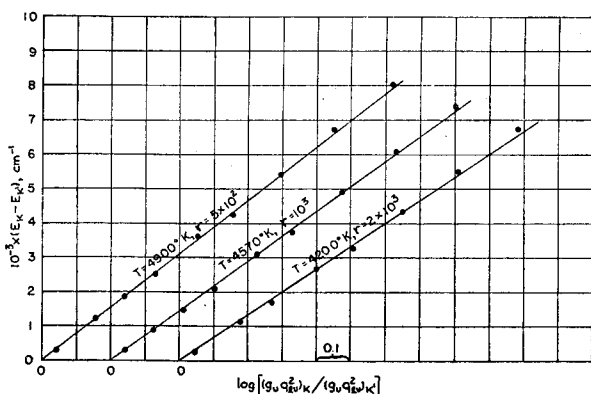


FIG. 12. Isointensity plots and apparent temperatures for $r = 5 \times 10^2$, 1×10^3 , and 2×10^3 .

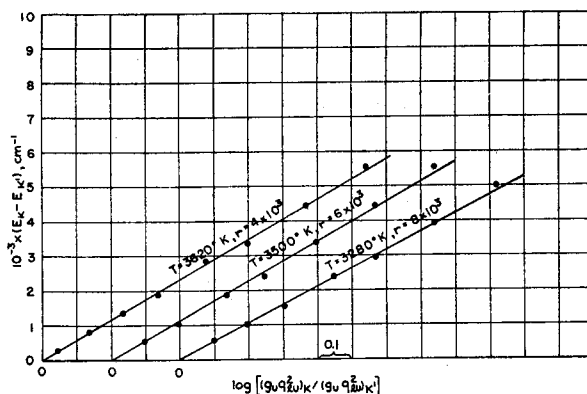


FIG. 13. Isointensity plots and apparent temperatures for $r = 4 \times 10^3$, 6×10^3 , and 8×10^3 .

A. Outline of Theory for Peak Intensities

Consider an isothermal region at temperature T with properties X , P_{\max} , $R(\nu_{lu})$, and $\epsilon = 1 - \exp(-P_{\max}X)$ which is observed through an isothermal region at temperature T' with properties X' , P_{\max}' , $R'(\nu_{lu})$, and $\epsilon' = 1 - \exp(-P_{\max}'X')$. The maximum observable intensity for the spectral line whose center lies at the frequency ν_{lu} is

$$I_{\max} = R(\nu_{lu}) \left\{ \epsilon + \left[\frac{\epsilon'}{1 - \epsilon'} \right] \times \exp(-h\nu_{lu}/k) \left[\frac{1}{T'} - \frac{1}{T} \right] \right\} (1 - \epsilon'). \quad (23)$$

A conventional plot for the study of emission experiments can be constructed according to the scheme outlined below.

- (1) For $T = 3000^\circ\text{K}$ and $T' = 1500^\circ\text{K}$ and fixed values of $\epsilon(K=1)$ and $\epsilon'(K=1)$ for the P_1 branch calculate $(P_{\max}X)_{K=1}$ and $(P_{\max}'X')_{K=1}$.
- (2) Calculate the ratios $S_{lu}(K, T)/S_{lu}(K=1, T)$ and $S_{lu}'(K, T')/S_{lu}'(K=1, T')$.
- (3) Calculate $(P_{\max}X)_K$ and $(P_{\max}'X')_K$ and hence $\epsilon(K)$ and $\epsilon'(K)$.
- (4) Determine I_{\max} from Eq. (23) and plot $\log[I_{\max}/(g_u q_{lu}^2)(\nu_{lu})^3]$ as a function of $E_u(K)$.

B. Discussion of Results for Peak Intensities

The results of numerical calculations are summarized in Figs. 14 and 15 for $\epsilon(K=1) = 0.3$ and 0.9 , respectively, for varying values of $\epsilon'(K=1)$ with $\epsilon'(K=1) \leq \epsilon(K=1)$. Reference to Figs. 14 and 15 clearly shows that observations through a cool isothermal region accentuate the distortion observed for self-absorption alone. For example, for $\epsilon(K=1) = \epsilon'(K=1) = 0.3$ a definite curvature is observed (see Fig. 14), whereas for $\epsilon(K=1) = 0.3$ and $\epsilon'(K=1) = 0$ a linear plot with a nearly "normal" temperature obtains (see Fig. 1). For strong self-absorption both in the hotter and cooler gas layers, extensive self-reversal may occur,¹¹ leading to no real values for the "temperature" (see Fig. 15).

¹¹ R. D. Cowan and G. H. Dieke, *Revs. Modern Phys.* **20**, 418 (1948).

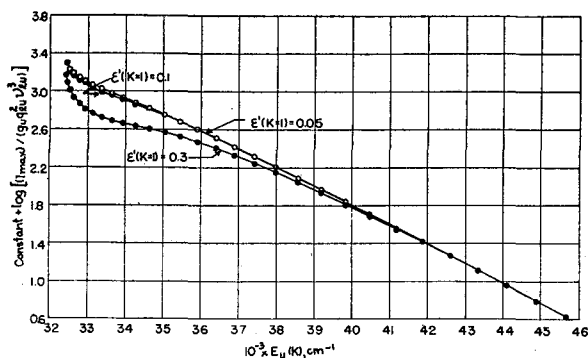


FIG. 14. Conventional plots for the interpretation of emission experiments with two adjacent isothermal regions at 1500 and 3000°K, respectively, for $\epsilon(K=1)=0.3$ for the P_1 branch.

It should perhaps be emphasized that the data shown in Figs. 14 and 15 are only of qualitative significance in so far as application to real flames is concerned. Furthermore, the results are, of course, modified if appropriate plots for total intensities are used instead of plots for peak intensities. In general, one would expect the extent of distortion to be somewhat diminished for total intensity measurements. Detailed calculations will not be presented here since the precise evaluation of the integrals involved is somewhat laborious and since the results would add little to the qualitative conclusions stated above.

VII. APPLICATION TO FLAMES

It is evident that none of the quantitative results presented for idealized systems in Secs. II to VI apply to real flames. Nevertheless, it is perhaps justifiable to perform some extrapolation to real systems.

To begin with, it is clear that observed "anomalies" can be explained by distortion of experimental data through self-absorption and/or temperature gradients. In order to make observable anomalies appear real, it is therefore necessary to perform experiments proving that distortion of data does not play a significant role. The proof should be direct and not inferential.

In order to emphasize the fact that inferential proof may be no proof at all, we consider, for example, an isothermal system at 3000°K with $\epsilon'(1)=0.70$ for the P_1 branch. Conventional interpretation of emission experiments (see Fig. 1) will then show experimental data which can be correlated by intersecting straight lines leading to a value of $T_u' \approx 5000^\circ\text{K}$ for the 2Σ state for $10 \leq K \leq 18$ (see Table I). Next, absorption experiments are performed with a light source at 8000°K, and considering the inevitable scatter of experimental data, the observed results are well correlated by a single straight line with $T_l' \approx 3650^\circ\text{K}$ (see Fig. 3). On the basis of these experimental results, one could argue with vigor for a nearly "normal" distribution of OH in the ground (2Π) state and for abnormal excitation of OH in the excited (2Σ) state. For the case under discussion, in

spite of the seemingly convincing inferential evidence, the conclusion would obviously be erroneous.

We have presented previously¹² a critical review of available experimental evidence for anomalous population temperatures in flames in which we emphasized the lack of unequivocal evidence either for or against the reality of the anomalies, noting, however, the wealth of inferential evidence, in favor of a nonequilibrium distribution of OH, presented by Gaydon and Wolfhard.¹ We did not necessarily intend to replace a temperature anomaly by a concentration anomaly. Rather we were primarily interested in showing that as yet the experimental evidence is not sufficiently clear to warrant quantitative interpretation. We have proposed a two-path method which eliminates all errors arising from self-absorption in *isothermal* systems for spectral lines with Doppler contour.¹³ However, we do not consider the method to be exactly valid for the study of regions of active combustion. The only conclusion which we feel justified in stating at the present time is that the spectroscopic study of regions of active combustion is useful for species identification and may, in time, lead to a valid quantitative picture, for example, of OH rotational temperatures and OH concentrations. The final analysis may prove or disprove the reality of anomalies. However, we shall find such proof convincing only if every precaution has been taken to eliminate instrumental errors and if all necessary corrections for distortions have been made by a realistic study of temperature gradients and of the extent of self-absorption. In this connection we wish to emphasize again the fact that the use of the iso-intensity method for the R_2 branch, with proper consideration for all of the precautions mentioned by Dieke,⁵ will minimize self-absorption errors. However, the use of the R_2 branch is not sufficient to eliminate the coupled effects of self-absorption and temperature gradients (compare with Sec. VI).

The question of the reality or fiction of anomalous rotational, vibrational, and electronic temperatures for OH in flames is of practical importance in connection

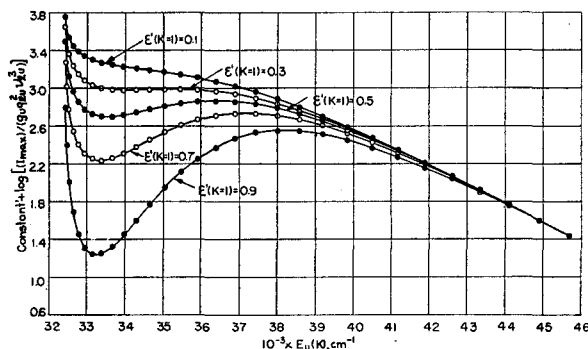


FIG. 15. Conventional plots for the interpretation of emission experiments with two adjacent isothermal regions at 1500 and 3000°K, respectively, for $\epsilon(K=1)=0.9$ for the P_1 branch.

¹² S. S. Penner, J. Chem. Phys. **20**, 1334 (1952).

¹³ S. S. Penner, J. Chem. Phys. **20**, 1341 (1952).

with the development of rigorous theories of one-dimensional laminar flame propagation.¹⁴ A review of observed anomalies shows uniformly high population temperatures not only for OH but also for other chemical species. On the other hand, theoretical studies by Golden and Peiser show a low rotational temperature for newly formed HBr.¹⁵ If nonequilibrium distributions persist in flames, the attempts at a rigorous calculation of burning velocities for one-dimensional flame propagation are enormously complicated because of our completely inadequate knowledge of detailed reaction mechanisms, particularly between molecules and radicals in excited states. The hypothesis that spectroscopic investigations yield information about side reactions and can therefore be ignored in a realistic formulation of the detailed reaction steps in flames is not altogether satisfying, since energy must be conserved and we have as yet no detailed knowledge concerning energy-deficient chemical species in the reaction zones of flames. For this reason, continued spectroscopic studies of flames are of interest not only in ascertaining details concerning the particular reaction steps which can be studied conveniently, but they also have a bearing on a parameter such as the linear burning velocity.

In conclusion, the author takes pleasure in expressing his appreciation to Dr. O. R. Wulf and Dr. H. S. Tsien for helpful comments. The numerical work was performed by E. K. Björnerud and R. W. Kavanagh.

APPENDIX I. BASIC RELATIONS IN TERMS OF TOTAL EMITTED INTENSITIES

The expressions given in Sec. II require slight modifications when total intensity ratios rather than peak intensity ratios are available. If the apparent integrated intensity of the spectral line with center at the frequency ν_{lu} is denoted by the symbol $A(\nu_{lu})$, then, as is well known,¹⁶

$$A(\nu_{lu}) \simeq R^0(\nu_{lu})(mc^2/2\pi kT_l \nu_{lu}^2)^{-1/2} (P_{\max} X) \times \left\{ \sum_{n=0}^{\infty} [(n+1)^{1/2}(n+1)!]^{-1} (-P_{\max} X)^n \right\}. \quad (\text{A1})$$

From Eqs. (1) and (A1) it follows that

$$I_{\max} = [A(\nu_{lu})/\nu_{lu}] (mc^2/2\pi kT_l)^{1/2} \xi, \quad (\text{A2})$$

where

$$\xi = \left\{ (P_{\max} X) \sum_{n=0}^{\infty} [(n+1)^{1/2}(n+1)!]^{-1} \times (-P_{\max} X)^n \right\}^{-1} [1 - \exp(-P_{\max} X)]. \quad (\text{A3})$$

¹⁴ J. O. Hirschfelder and C. F. Curtiss, *J. Chem. Phys.* **17**, 1076 (1949).

¹⁵ S. Golden and A. M. Peiser, *J. Chem. Phys.* **17**, 630 (1949).

¹⁶ R. Ladenburg, *Z. Physik* **65**, 200 (1930).

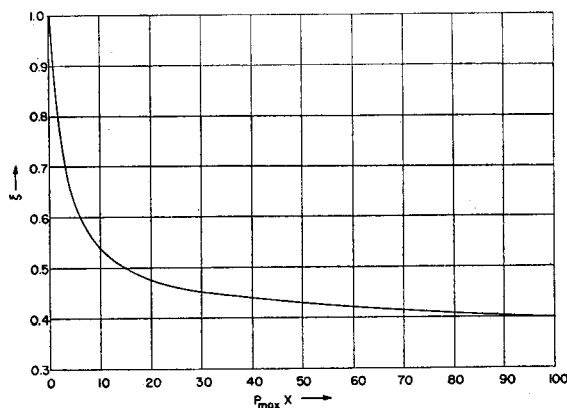


FIG. 16. The quantity ξ as a function of $P_{\max} X$.

Since $\xi=1$ for $P_{\max} X \ll 1$, it is apparent from Eqs. (7) and (A2) that

$$\frac{\partial \ln[A(\nu_{lu})/\nu_{lu}^4 g_u(q_{lu})^2]}{\partial E_u} = -\frac{1}{kT_u}$$

for $\epsilon' \ll 1$ for all lines. (A4)

Equation (A4) is the expression which is usually employed for the interpretation of experimental data. The value of ξ is plotted as a function of $P_{\max} X$ in Fig. 16.

When conventional plots for the determination of population temperatures are constructed according to Eq. (A4) for arbitrary values of $\epsilon'(1)$, results substantially equivalent to those shown in Fig. 1 are obtained. In this case the quantity $A(\nu_{lu})$ can be calculated from Eq. (A2) after obtaining I_{\max} by use of the procedure described in Sec. IIB.

APPENDIX II. POPULATION TEMPERATURES BASED ON APPARENT TOTAL ABSORPTION MEASUREMENTS FOR SPECTRAL LINES WITH DOPPLER CONTOUR

It is readily shown that the apparent total absorption A_T is related to the peak absorption A_{\max} through the expression

$$A_{\max} = A_T \cdot \xi \cdot (\nu_{lu})^{-1} (mc^2/2\pi kT_l)^{1/2}, \quad (\text{A5})$$

where ξ is given by Eq. (A3). By the use of Eqs. (A3) and (A5) it is a simple matter to convert the data given in Figs. 4 to 7 to the corresponding plots involving A_T . The values of ξ as a function of $P_{\max} X$ have been given in Fig. 16. Conclusions derived from conventional plots do not differ significantly from the material given in Sec. III, for the range of spectral emissivities considered in the present analysis.